



Published in final edited form as:

*Anal Chem.* 2012 January 17; 84(2): 1098–1103. doi:10.1021/ac202757c.

## A Wash-free, Electrochemical Platform for the Quantitative, Multiplexed Detection of Specific Antibodies

Ryan J. White<sup>a,e</sup>, Hannah M. Kallewaard<sup>a</sup>, Wen Hsieh<sup>b</sup>, Adriana S. Patterson<sup>a</sup>, Jesse B. Kasehagen<sup>d</sup>, Kevin J. Cash<sup>g</sup>, Takanori Uzawa<sup>f</sup>, H. Tom Soh<sup>b</sup>, and Kevin W. Plaxco<sup>a,c,\*</sup>

<sup>a</sup>Department of Chemistry and Biochemistry, University of California, Santa Barbara, CA 93106-9510

<sup>b</sup>Department of Mechanical Engineering, University of California, Santa Barbara, CA, 93106

<sup>c</sup>Graduate Program in Biomolecular Science and Engineering, University of California, Santa Barbara, CA, 93106

<sup>d</sup>Department of Sciences, Santa Barbara Middle School, Santa Barbara, CA, 93103

<sup>e</sup>Current Address: Department of Chemistry and Biochemistry, University of Maryland Baltimore County, 1000 Hilltop Circle, Baltimore, MD, 21250

<sup>g</sup>Current Address: Department of Pharmaceutical Sciences, Northeastern University, 360 Huntington Ave., 110 Mugar Life Sciences Building, Boston, MA 02115

<sup>f</sup>Current Address: RIKEN, Nano Medical Engineering Laboratory, 2-1 Hirosawa, Wako, Saitama, 351-0198 Japan

### Abstract

The diagnosis, prevention, and treatment of many illnesses, including infectious and autoimmune diseases, would benefit from the ability to measure specific antibodies directly at the point of care. Thus motivated, we designed a wash-free, electrochemical method for the rapid, quantitative detection of specific antibodies directly in undiluted, unprocessed blood serum. Our approach employs short, contiguous polypeptide epitopes coupled to the distal end of an electrode-bound nucleic acid “scaffold” modified with a reporting methylene blue. The binding of the relevant antibody to the epitope reduces the efficiency with which the redox reporter approaches, and thus exchanges electrons with, the underlying sensor electrode, producing readily measurable change in current. To demonstrate the versatility of the approach we fabricated a set of six such sensors, each aimed at the detection of a different monoclonal antibody. All six sensors are sensitive (sub-nanomolar detection limits), rapid (equilibration time constants ~8 min), and specific (no appreciable cross reactivity with the targets of the other five). When deployed in a millimeter-scale, an 18-pixel array with each of the six sensors in triplicate, support the simultaneous measurement of the concentrations of multiple antibodies in a single, sub-milliliter sample volume. The described sensor platform thus appears to be a relatively general approach to the rapid and specific quantification of antibodies in clinical materials.

### Introduction

The detection of multiple specific antibodies plays a central role in the diagnosis of infection, and the detection and monitoring of rheumatic and other autoimmune diseases.<sup>1-13</sup> The use of these as diagnostic markers is hampered, however, by limitations

\*Corresponding author, kwp@chem.ucsb.edu.

inherent in existing methods for antibody detection. Current standard methods for the detection of antibodies, including, for example, enzyme-linked immunosorbent assays (ELISA) and Western blots, are slow, cumbersome, laboratory-bound processes that require hours to days to return clinically actionable information.<sup>3</sup> Given that reduction in the time required to diagnosis disease speeds treatment, reduces complications and saves lives, technologies that move antibody detection from central clearing house laboratories to the point of care could dramatically improve patient outcomes in both the developed and developing worlds.<sup>13</sup>

In response to the need for point-of-care antibody detection recent years have seen the development of the lateral flow (“dipstick” or “rapid test”) assay.<sup>13,14</sup> This approach, which utilizes immobilized antigens, enzyme- or modified gold-nanoparticles with secondary antibodies, and a clever, wicking-based automated wash protocol to detect specific antibodies, has revolutionized, for example, the point-of-care detection of HIV infection.<sup>14</sup> Unfortunately, however, lateral flow assays at best provide only qualitative or semi-quantitative information regarding the serum levels of their targeted antibodies.<sup>9</sup> This limitation renders the approach poorly suited for use in monitoring autoimmune status and disease progression,<sup>15,16</sup> or for discriminating between active and prior infections.<sup>14,17</sup> Lateral-flow assays have also proven difficult to parallelize,<sup>9</sup> rendering them cumbersome in applications for which multiple antibodies must be monitored simultaneously.<sup>4,10</sup> There thus remains an important medical need for the *rapid, quantitative, multiplexed* measurement of antibody concentrations at the point of care.<sup>13,14</sup>

In an effort to meet this need, a number of reagent- and wash-free sensors have been reported that, at least in theory, could meet the significant challenges associated with this application (see for example ref 3). The large majority of these, however, including surfaceplasmon resonance- (SPR), quartz crystal microbalance- (QCM), field-effect transistor- (FET), microcantilever- and electrochemical impedance spectroscopy (EIS)-based approaches, fail when challenged with unprocessed clinical materials due to the non-specific adsorption of interferents. Consistent with this, none of these approaches have yet penetrated clinical laboratories, much less the point of care. Indeed, to date no general method for the quantitative detection of specific antibodies achieves diagnostically relevant sensitivity and specificity without relying on significant sample preparation, cumbersome laboratory equipment or highly trained personnel.<sup>14</sup> Here, in contrast, we demonstrate a quantitative, electrochemical platform for the rapid, wash-free detection of multiple specific antibodies directly in sub-milliliter clinical samples.

Our approach, which we have termed E-DNA (electrochemical DNA – a class of sensors employing redox-tagged, electrode-bound nucleic acid probes) antibody sensor (Fig. 1, *left*), employs a modified nucleic acid duplex as its signaling and recognition probe.<sup>19,20</sup> One strand of this probe (the anchor strand) is modified with a redox reporter (here methylene blue) at its 3' terminus and is affixed to an interrogating electrode via its 5' terminus. The second strand of the duplex probe (the recognition strand) is modified with the relevant antigen at its 5' terminus, placing this recognition element distal from the electrode. In the absence of the target antibody, the methylene blue approaches the electrode surface, allowing for efficient electron transfer. The binding of an antibody to the epitope impedes this approach, reducing the observed electron transfer efficiency (Fig. 1, *right*) and leading to a large readily measurable change in faradaic current (Fig. 1, *bottom*). To date we have described two E-DNA antibody sensors, both of which achieve nanomolar detection limits and are sufficiently selective to deploy directly in complex sample matrices such as crude soil extract, seawater and diluted blood serum.<sup>19,20</sup> These prior examples, however, both employed simple, small molecule haptens (digoxigenin and dinitrophenol) as their recognition elements, limiting their usefulness.<sup>19,20</sup> Here, in contrast, we demonstrate the

utility of the E-DNA antibody detection platform for the rapid, specific, multiplex detection of anti-protein antibodies.

The detection of anti-protein antibodies requires that we modify the E-DNA platform to present polypeptide recognition elements. To facilitate this we have employed a peptide nucleic acid (PNA)-based recognition strand; the peptide-bond backbone of PNA supports the ready solid-phase synthesis of PNA-polypeptide chimeras that both present the relevant epitope and can hybridize to our DNA anchor strand.<sup>21,22</sup> As an initial test of the utility of PNA/polypeptide chimeras in the E-DNA platform –and, indeed, the viability of using the approach to detect anti-polypeptide antibodies– we employed a 25-base PNA recognition strand terminated with the well-characterized, eight-residue FLAG epitope (with two glycines added to act as spacers: DYKDDDDKGG-PNA), a commonly used affinity tag for antibody-based protein purification.<sup>23</sup>

## Experimental

### Materials

6-mercapto-1-hexanol, fibrinogen (from bovine plasma), bovine serum albumin, tris(2-carboxyethyl)phosphine, anti-FLAG antibody (Sigma Aldrich), Tween 20 (Acros), and all other antibody targets (Polymun Scientific - Vienna, Austria) were all used as received. Dulbecco's phosphate buffered saline 20X stock (Sigma Aldrich) was diluted to 1X or 3X final concentrations and brought to pH 7.4. All antibodies were used as received. The 5'-thiol-, 3'-methylene blue-modified DNA anchor strand (HPLC-purified, Biosearch Technologies, Inc. -Novato, CA) was used as received without further purification. The anchor strand sequence was 5' – d Thiol C6 SS – GCAGTAACAAGAATAAAACGCACTGC – Methylene Blue – 3'. The peptide nucleic acid – peptide epitope chimera (HPLC-purified, Panagene – Daejeon, Korea) were also used without further purification. Each sequence followed the model EPITOPE-cagtggcgtttattctgttactg, with lower case letters representing PNA nucleosides.

### Sensor Fabrication

Sensors are prepared using a previously reported protocol<sup>24</sup> with minor alterations. In brief, gold rod electrodes (2 mm diameter, CH Instruments, Austin, TX) were first mechanically polished in a slurry of diamond paste (Buehler, Lake Bluff, IL) in ethanol followed by sonication in ethanol for 5 min. This was followed by polishing with a slurry of 50 nm aluminum oxide in water (Buehler, Lake Bluff, IL) and then sonication in water for 5 min. The electrodes were further cleaned by first voltammetric scans in 0.5 M NaOH to remove any organic surface contamination and then a series of oxidative and reductive scans in 0.5 M H<sub>2</sub>SO<sub>4</sub> and then 0.1 M H<sub>2</sub>SO<sub>4</sub>/0.01 M KCl as previously described (30). Electrode area was determined by integration of the gold oxide reduction peak in 0.05 M H<sub>2</sub>SO<sub>4</sub>. After physical cleaning of the electrode surface, electrodes were rinsed thoroughly and immersed in 25 nM (determined using absorbance at 260 nm) anchor strand DNA for 1 h in Dulbecco's phosphate buffered saline, pH 7.4. Prior to this the DNA anchor strand had been left in 10 mM tris(2-carboxyethyl)phosphine for 1 h to reduce any disulfides formed by the thiol-modified DNA. After immobilization of the anchor strand DNA, to passivate the remaining electrode area sensors were rinsed and immersed for 1 h in 3 mM 6-mercapto-1-hexanol in the same buffer. To create the DNA anchor strand/PNA recognition strand duplex on the surface, sensors were incubated in a 100 nM solution of the recognition strand overnight (~12 h) in, once again, the same Dulbecco's buffer. Finally, to further block non-specific adsorption and ensure good performance in blood serum the sensors were immersed in a 1 M NaCl with 0.1% (wt/wt) bovine serum albumin and 0.05% (v/v) tween 20 prior to use.

## Sensor Operation

Squarewave voltammetry was performed using a three-electrode setup on a CH Instruments electrochemical workstation with a step potential of 0.001 V, an amplitude 0.025 V and a frequency of 60 Hz. All titrations were performed in the same blocking solution as described above.

## Multi-Sensor Array Chip Fabrication and Measurements

The microfabricated chips employ eighteen gold working electrodes, and a common platinum quasi-reference and a platinum counter electrode. The electrodes were fabricated based on previously described method.<sup>25</sup> Briefly, platinum reference and counter electrodes and gold working electrodes were sequentially microfabricated on a 4"-diameter, 500- $\mu\text{m}$ -thick borofloat glass wafer (Mark Optics, Santa Ana, CA) through successive standard lift-off processes. The lift-off consisted of transparency mask (Grayphics, Santa Barbara, CA) based contact photolithography, electron-beam evaporation based metal deposition (180 nm of platinum or gold on 20 nm titanium for adhesion; VES 2550, Temescal, Livermore, CA), and immersion and gentle sonication in acetone. The electrode wafer was finally diced (Disco DAD-2H/6, Tokyo, Japan) into individual chips, each measuring 25.4 mm by 25.4 mm. To ensure efficient reagent handling during experimentation, a disposable PDMS chamber was attached to the electrode chip to define a reaction well. The PDMS chambers were cut from a 250- $\mu\text{m}$ -thick PDMS sheet (BISCO Silicones, Rogers Corporation, Carol Stream, IL) with a programmable sign-cutting tool (CE5000-60, Graphtec, Santa Ana, CA). The gold working electrode pixels were electrochemically cleaned prior to anchor strand deposition using a series of cyclic voltammetric scans in 0.05 M  $\text{H}_2\text{SO}_4$ . Sensor fabrication and measurement was then performed as described above using a blocking buffer comprising a 3X Dulbecco's phosphate buffered saline, 0.1% (wt:wt) bovine fibrinogen and 0.05% (v:v) tween 20.

## Results and Discussion

Our anti-FLAG antibody sensor rapidly and sensitively recognizes its target antibody (Fig. 2). Specifically, by measuring the percent change in faradaic peak current (with respect to the unbound state) as measured with square wave voltammetry the sensor readily detects anti-FLAG antibody at concentrations as low as 500 pM (Fig. 3 – *top left*). Titration with increasing concentrations of the FLAG antibody results in a signal change that rises monotonically with a dissociation constant within error of the  $\sim 3$  nM reported against the FLAG peptide displayed on a cell surface.<sup>26,27</sup> The anti-FLAG antibody sensor responds rapidly to its target, exhibiting an equilibration time constant of  $\sim 8$  min at room temperature and exhibiting an appreciable change in signal after just 2 min incubation with its target (Fig. 2 – *top*). The sensor is also specific and selective. For example, we do not observe any significant signal change (i.e., within typical standard errors of  $\sim 5\%$ ) when we challenge the sensor with 50 nM of mixed, non-specific IgG antibodies (Fig. 2 – *bottom*). Finally, the sensor is selective and performs well even when the target antibody is presented in undiluted blood serum (Fig.1), or in whole blood diluted 1:4 with buffered saline (Fig. S1).

The E-DNA antibody detection platform appears applicable to the detection of a wide range of antibodies. To demonstrate this capability, we first selected five monoclonal anti-HIV antibodies from the literature to use as a test bed to determine the likelihood that we can build a sensor for the detection of any given antibody. We selected these antibodies using only the following criteria: 1) the antibody must be directed against a relatively short (limit arbitrarily set at 20-residues) contiguous epitope (a continuous polypeptide chain), 2), the solution-phase binding must be well characterized, and 3) the antibody must be commercially available. Our selection of antibodies, thus, was based on their technical and

programmatic convenience rather than their clinical interest. Nonetheless, using this approach we selected a set of antibodies to serve as at least an initial test of the generalizability of the E-DNA antibody sensor approach. The five antibodies in this set (Table 1) all bind specific, well-characterized HIV epitopes of 6 to 18 residues with dissociation constants below 5 nM.<sup>28-33</sup>

Out of our first set of five anti-HIV antibody sensors we achieved three successes. That is, three of our five initial sensors supported the rapid and specific detection of their target antibodies at sub-nanomolar concentrations, a detection limit that compares well with the 1-10 nM serum concentrations reported for, for example, clinically relevant anti-HIV antibodies.<sup>34</sup> Even at antibody concentrations as high as 40 nM, however, sensors based on the 4E10 and p17 epitopes of HIV failed to respond to their targets (Fig. S2). Fortunately, further evaluation of the literature suggested that small alterations in the sequences of either epitope (illustrated in Table 1) drastically affect its binding affinity.<sup>29,30</sup> For example, with the addition of a poly-lysine tail to improve solubility the reduction of the 4E10 epitope to the shortest linear sequence that exhibits affinity to the anti-4E10 antibody significantly improves its binding constant.<sup>30</sup> Armed with this knowledge we fabricated new sensors employing slightly modified versions of these two epitopes (see Table 1) and found that, once again, these support the rapid, sub-nanomolar detection of their target antibodies (Fig. 3). We thus ultimately achieved the sensitive and specific detection of all five of the anti-HIV antibodies in our test set (Fig. 3), suggesting that the E-DNA antibody detection approach is quite versatile. Indeed, including our anti-FLAG antibody sensor we have achieved a six-for-six success rate, and thus, at least for antibodies that bind short, contiguous epitopes, the E-DNA antibody detection approach may be nearly universal.

Consistent with their sub-nanomolar detection limits, all six of our sensors exhibit reasonably high signal gain (Fig. 3). Specifically, at saturating target concentrations four of the six exhibit a ~40% change in relative signaling current and two exhibit 60 to 75% changes. The origins of the larger gains of the latter two sensors is unclear, but the results are highly reproducible for each epitope we have employed. We thus suspect that the variation in gain from epitope to epitope arises due to the specific geometry of the relevant epitope/antibody complex.

The ability to perform multiplexed detection would offer significant advantages for point of care diagnostics in that it allows for the simultaneous monitoring of multiple markers in a single sample. Such multiplexing likewise supports the performance of both negative and positive controls in that same sample. Together these attributes can significantly improve the specificity and sensitivity with which diseases such as systemic lupus erythematosus, for which no single antibody test achieves acceptable clinical specificity,<sup>4</sup> are detected and diagnosed. Motivated by these observations we integrated our six sensors in a single, multiplexed device employing gold electrodes microfabricated on a glass substrate. Our devices contained eighteen  $500 \times 500 \mu\text{m}$  gold working electrodes arrayed in six, three-pixel clusters (Fig. 4 - *top*). To convert these chips into a sensor array we first deposited a common anchor strand sequence on all 18 pixels. We then modified each three-pixel cluster with one of the specific recognition probes yielding a device that can perform simultaneous, triplicate measurements of each of six antibody targets.

Our multi-sensor arrays readily support the simultaneous detection multiple of antibodies in a single, sub-milliliter sample volume. For example, when we challenge our array with a mixture of anti-FLAG, 2F5 and 4B3 antibodies at 25 nM (each), the appropriately labeled pixels—and only the appropriately labeled pixels—respond accordingly (Fig. 4 - *bottom*) with little ( ~3% signal change) crosstalk being observed for the other pixels. Moreover, we have accomplished this detection in a few minutes, with a convenient, wash-free device, and

using only a modest, 200  $\mu$ l sample volume. Of note, the gain differs somewhat between sensors fabricated on the gold disc electrodes described above and on the microfabricated electrodes described here. We attribute this to differences in the surface morphology of the gold electrodes.<sup>19,20</sup> Sensor performance is highly dependent of probe packing density on the sensor surface therefore differences in morphology in the sensor surface between the hand-polished disc electrodes and smoother microfabricated surfaces may lead to difference packing densities using the same thiolated-DNA concentration.<sup>35</sup> The DNA modification concentration (and thus optimal packing density) for the latter surface was not optimized to achieve maximum signal change.

## Conclusion

Here we have demonstrated a multiplexed electronic device for the quantitative measurement of anti-protein antibodies in a single, sub-milliliter sample. Our approach is rapid (minutes), sensitive (sub-nanomolar), and convenient (single-step, wash-free). Moreover, because signal generation in the E-DNA platform is predicated on specific, target-induced changes in collision efficiency, our sensors are relatively insensitive to nonspecific adsorption and can be deployed directly in complex clinical materials. The electrochemical readout of our sensor platform is likewise facile, and is supported by simple, inexpensive electronics well suited for deployment outside of the laboratory.<sup>36</sup> Finally, the platform appears general, at least for the detection of antibodies against contiguous epitopes: we ultimately developed high affinity, high-specificity sensors against all six of the monoclonal antibody targets in our initial test set. Taken together, these attributes suggest the E-DNA antibody platform may be prove a promising approach for the quantitative detection of antibodies directly at the point of care.

## Supplementary Material

Refer to Web version on PubMed Central for supplementary material.

## Acknowledgments

The authors wish to acknowledge funding from the Bill and Melinda Gates Foundation (KWP), the NIH (GM062958-01 to KWP) and a fellowship by National Institutes of Health under Ruth L. Kirschstein National Research Service Award (1 F32 GM087126-01A1 to R.J.W.)

## References

- (1). Baud D, Regan L, Greub G. *Eur. J. Clin. Microbiol. Infect.* 2010; 29:669–75.
- (2). Burbelo PD, Issa AT, Ching KH, Cohen JI, Iadarola MJ, Marques A. *Clin. Vaccine Immunol.* 2010; 17:904–909. [PubMed: 20392886]
- (3). Chan CP, Cheung Y, Renneberg R, Seydack M. *Adv. Biochem. Eng. Biotechnol.* 2008; 109:123–54. [PubMed: 17874052]
- (4). Gill JM, Quisel AM, Rocca PV, Walters DT. *Am. Fam. Physician.* 2003; 68:2179–86. [PubMed: 14677663]
- (5). Murray CK, Gasser RA, Magill AJ, Miller RS. *Clin. Microbiol. Rev.* 2008; 21:97–110. [PubMed: 18202438]
- (6). Korponay-Szabó IR, Szabados K, Pusztai J, Uhrin K, Ludmány E, Nemes E, Kaukinen K, Kapitány A, Koskinen L, Sipka S, Imre A, Mäki M. *British Medical Journal.* 2007; 335:1244–7. [PubMed: 18063612]
- (7). Parekh BS, Kennedy MS, Dobbs T, Pau C-P, Byers R, Green T, Hu DJ, Vanichseni S, Young NL, Choopanya K, Mastro TD, McDougal JS. *AIDS Res. Hum. Retroviruses.* 2002; 18:295–307. [PubMed: 11860677]
- (8). Pfäfflin A, Schleicher E. *Anal.Bioanal. Chem.* 2009; 393:1473–80. [PubMed: 19104782]

- (9). Posthuma-Trumpie GA, Korf J, van Amerongen A. *Anal. Bioanal. Chem.* 2009; 393:569–82. [PubMed: 18696055]
- (10). Brennan DJ, O'Connor DP, Rexhepaj E, Ponten F, Gallagher WM. *Nat. Rev. Cancer.* 2010; 10:605–17. [PubMed: 20720569]
- (11). Tang R, Yeh C, Wang J-Y, Changchien C, Chen J-S, Hsieh L. *Ann. Surg. Oncol.* 2009; 16:2516–2523. [PubMed: 19565285]
- (12). Rouquette A-M, Desgruelles C, Laroche P. *Am. J. Clin. Pathol.* 2003; 120:676–681. [PubMed: 14608892]
- (13). Bissonnette L, Bergeron MG. *Clin. Microbiol. Infect.* 2010; 16:1044–1053. [PubMed: 20670286]
- (14). Yager P, Domingo GJ, Gerdes J. *Annu. Rev. Biomed. Eng.* 2008; 10:107–44. [PubMed: 18358075]
- (15). Osterland CK. *Clin. Chem.* 1994; 40:2146–2153. [PubMed: 7955401]
- (16). Nakamura M, Shimizu-Yoshida Y, Takii Y, Komori A, Yokoyama T, Ueki T, Daikoku M, Yano K, Matsumoto T, Migita K, Yatsuhashi H, Ito M, Masaki N, Adachi H, Watanabe Y, Nakamura Y, Saoshiro T, Sodeyama T, Koga M, Shimoda S, Ishibashi H. *J. Hepatology.* 2005; 42:386–392.
- (17). Goudsmit J, Lange JMA, Paul DA, Dawson GJ, The S, Diseases I, Mar N. *Infection.* 1987; 155:558–560.
- (18). Giljohann DA, Mirkin CA. *Nature.* 2009; 462:461–4. [PubMed: 19940916]
- (19). Cash KJ, Ricci F, Plaxco KW. *J. Am. Chem. Soc.* 2009; 131:6955–6957. [PubMed: 19413316]
- (20). Cash KJ, Ricci F, Plaxco KW. *Chem. Commun.* 2009:6222–6224.
- (21). Egholm M, Buchardt O, Christensen L, Behrens C, Freier SM, Driver DA, Berg RH, Kim SK, Norden B, Nielsen PE. *Nature.* 1993; 365:566–8. [PubMed: 7692304]
- (22). Lee H, Jeon JH, Lim JC, Choi H, Yoon Y, Kim SK. *Org. Lett.* 2007; 9:3291–3293. [PubMed: 17661472]
- (23). Hopp TP, Prickett KS, Price VL, Libby RT, March CJ, Cerretti DP, Urdal DL, Conlon PJ. *Nat. Biotech.* 1988; 6:1204–1210.
- (24). Xiao Y, Lai RY, Plaxco KW. *Nature Protoc.* 2007; 2:2875–80. [PubMed: 18007622]
- (25). Ferguson BS, Buchsbaum SF, Swensen JS, Hsieh K, Lou X, Soh HT. *Anal. Chem.* 2009; 81:6503–8. [PubMed: 19586008]
- (26). Wegner GJ, Lee HJ, Corn RM. *Anal. Chem.* 2002; 74:5161–5168. [PubMed: 12403566]
- (27). Firsov D. *Proc. Natl. Acad. Sci. USA.* 1996; 93:15370–15375. [PubMed: 8986818]
- (28). Barbato G, Bianchi E, Ingallinella P, Hurni WH, Miller MD, Ciliberto G, Cortese R, Bazzo R, Shiver JW, Pessi A. *J. Mol. Biol.* 2003; 330:1101–1115. [PubMed: 12860131]
- (29). Conley AJ, Kessler JA, Boots LJ, Tung JS, Arnold BA, Keller PM, Shaw AR, Emimi EA. *Proc. Natl. Acad. Sci. USA.* 1994; 91:3348–3352. [PubMed: 7512731]
- (30). Brunel FM, Zwick MB, Cardoso RMF, Nelson JD, Wilson IA, Burton DR, Dawson PE. *J. Virol.* 2006; 80:1680–1687. [PubMed: 16439525]
- (31). Papsidero LD, Sheu M, Ruscetti FW. *J. Virol.* 1989; 63:267–272. [PubMed: 2462060]
- (32). Palacios-Rodriguez Y, Gazarian T, Rowley M, Majluf-Cruz A, Gazarian K. *J. Microbiol. Methods.* 2007; 68:225–235. [PubMed: 17046088]
- (33). Ota A, Ueda S. *Hybridoma.* 1998; 17:471–477. [PubMed: 9873993]
- (34). Steindl F, Armbruster C, Pierer K, Purtscher M, Kattinger HW. *J. Immunol. Methods.* 1998; 217:143–51. [PubMed: 9776584]
- (35). Love JC, Estroff LA, Kriebel JK, Nuzzon RG, Whitesides GM. *Chem. Rev.* 2005; 105:1103–1169. [PubMed: 15826011]
- (36). Rowe AA, Bonham AJ, White RJ, Zimmer MP, Yadgar RJ, Hobza TM, Honea JW, Ben-Yaacov I, Plaxco KW. *PLoS One.* 2011; 6:e23783. [PubMed: 21931613]

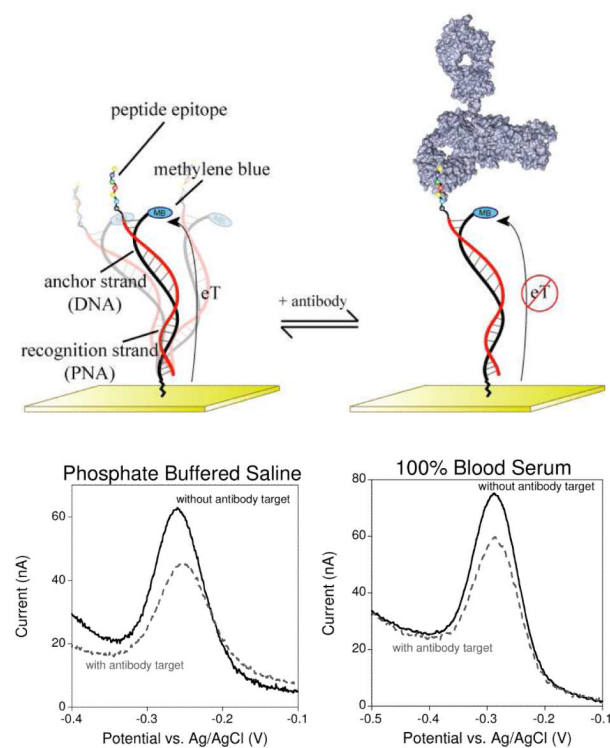


**Figure 1.**

The E-DNA antibody sensor (*top*) comprises an electrode-bound, redox-reporter-modified DNA strand, termed the “anchor strand,” that forms a duplex with a complementary “recognition strand” (here composed of PNA) to which the relevant recognition element is covalently attached. In the absence of antibody binding (*top left*) the flexibility of the surface attachment chemistry supports relatively efficient electron transfer between the redox reporter and the electrode surface. Binding to the relevant target antibody (*top right*) decreases electron transfer, presumably by reducing the efficiency with which the reporter collides with the electrode. (*Bottom*) Binding can thus be measured as a decrease in peak current as observed via square wave voltammetry. As shown, sensors in this class are highly selective and perform equally well in buffered saline (*bottom left*), undiluted blood serum (*bottom right*), or 1:4 diluted whole blood (see Fig. S1).



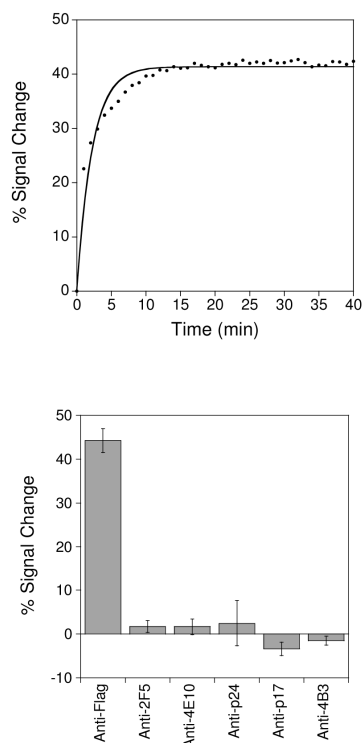


**Figure 2.**

E-DNA antibody sensors respond rapidly and specifically to their targets. (*top*) A sensor for the detection of anti-FLAG antibodies, for example, equilibrates with a time constant of  $\sim 8$  min at, as shown, to addition of 25 nM antibody at 25°C. (*bottom*) This same sensor does not produce a significant response ( $<5\%$  signal change, which is within normal sensor-to-sensor variability) to any of the other five antibodies employed elsewhere in this work. Error bars represent the standard deviation of at least 3 independently fabricated sensors, and are dominated by sensor-to-sensor fabrication variability.

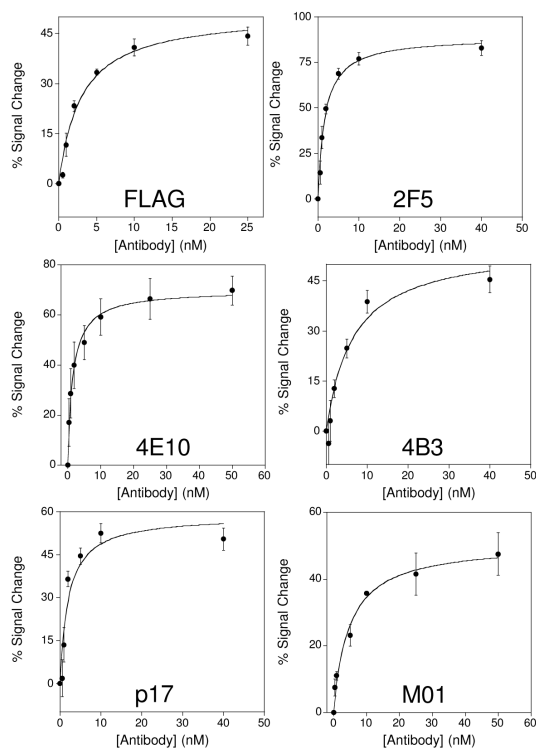


**Figure 3.**

The E-DNA approach appears a general method for the quantitative detection of antibodies directed against contiguous epitopes. Shown are the responses of the anti-FLAG antibody sensor and five additional sensors directed against antibodies that bind specific, contiguous epitopes derived from HIV. All six sensors achieve sub-nanomolar detection limits. Error bars represent the standard deviation of measurements made using at least three independently fabricated sensors.

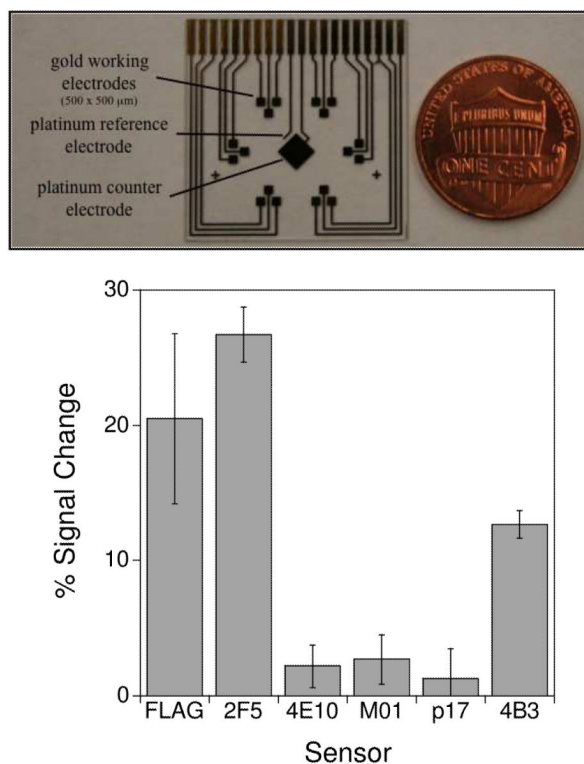


**Figure 4.**

The electrochemical E-DNA antibody sensor readily supports multiplexed detection. Here we have employed a microfabricated chip (*top*) containing eighteen  $500 \times 500 \mu\text{m}$  sensors arranged in six, three-pixel clusters. Each cluster is directed against a different antibody, and thus the device supports the simultaneous, triplicate measurement of six different targets. A sample well is placed on top of this chip to complete the sensor. (*bottom*) When this device is challenged with  $200 \mu\text{l}$  of a mixture of anti-FLAG, anti-2F5 and anti-4B3 antibodies (here at 25 nM), only the appropriate pixels exhibit any significant signal change. Error bars represent the standard deviation of measurements made on each of the three specifically labeled pixels.

**Table 1**

The epitopes employed here

Epitope Target	Epitope Sequence	Previously Reported <sup>a</sup> K <sub>d</sub> (nM)	Observed K <sub>d</sub> (nM)	Sensor Gain <sup>b</sup>
FLAG	DYKDDDDKGG	3 nM	3.0 ± 0.5 nM	-45%
HIV gp41 (4B3)	LWGCSGKLVCTT	Not reported	7 ± 2nM	-45 ± 4%
HIV gp41 (2F5)	ELLELDKWASLWNC	0.77 nM	1.7 ± 0.2 nM	-83 ± 4%
HIV gp41 (4E10)	CSLWNWFNITNWLWYIKC	20.2 nM	N/A	N/A
	NWFDITNWLWYIKKKK	20 nM	1.6 ± 0.2 nM	-70 ± 6%
HIV p17 (32/1.24.89)	GKIRLRPG	Not reported	N/A	N/A
	EKIRLR	200 pM	2 ± 1 nM	-50 ± 6%
HIV p24 (M01)	GATPQDLNTML	Not reported	5 ± 1 nM	-47 ± 6%

<sup>a</sup>Taken from the following references: FLAG(26,27), 2F5(28,29), 4E10(30), p17(31,33), 4B3(32), M01(34).

<sup>b</sup>Relative signal change observed at saturating (40 nM) antibody concentration. Confidence intervals represent the standard deviation of at least three independently fabricated sensors.